

UNCLASSIFIED

AD NUMBER

AD314095

CLASSIFICATION CHANGES

TO: UNCLASSIFIED

FROM: CONFIDENTIAL

LIMITATION CHANGES

TO:
Approved for public release; distribution is unlimited. Document partially illegible.

FROM:
Distribution authorized to U.S. Gov't. agencies and their contractors;
Administrative/Operational Use; JAN 1960. Other requests shall be referred to Arnold Engineering Development Center, Arnold AFB, TN. Document partially illegible.

AUTHORITY

AEDC ltr Aug 1973; AEDC Ltr Aug 1972

THIS PAGE IS UNCLASSIFIED

UNCLASSIFIED

AD NUMBER

AD314095

CLASSIFICATION CHANGES

TO:

CONFIDENTIAL

FROM:

SECRET

AUTHORITY

31 Jan 1972, DoDD 5200.10

THIS PAGE IS UNCLASSIFIED



AD

314095

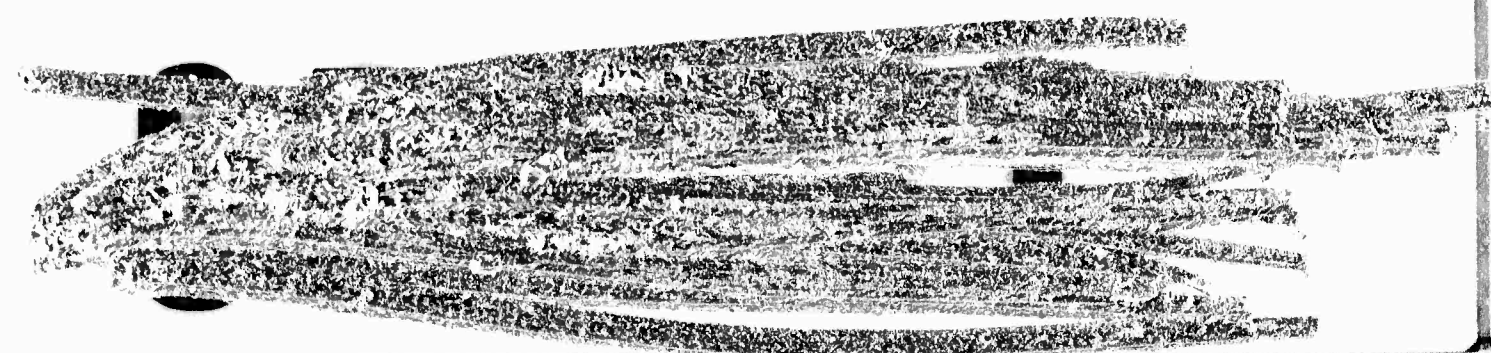
**FOR
MICRO-CARD
CONTROL ONLY**

1 OF 1

Reproduced by

Armed Services Technical Information Agency

ARLINGTON HALL STATION; ARLINGTON 12 VIRGINIA



"NOTICE: When Government or other drawings, specifications or other data are used for any purpose other than in connection with a definitely related Government procurement operation, the U.S. Government thereby incurs no responsibility, nor any obligation whatsoever; and the fact that the Government may have formulated, furnished, or in any way supplied the said drawings, specifications or other data is not to be regarded by implication or otherwise as in any manner licensing the holder or any other person or corporation, or conveying any rights or permission to manufacture, use or sell any patented invention that may in any way be related thereto."

15

314095
D.N.O.

STIA FILE COPY



(TITLE UNCLASSIFIED)



**STABILITY AND CONTROL CHARACTERISTICS
OF SEVEN LENTICULAR MODELS
AT MACH NUMBER 5**

By
A. Anderson
VKF, ARO, Inc.

FC

January 1960



**ARNOLD ENGINEERING
DEVELOPMENT CENTER**

AIR RESEARCH AND DEVELOPMENT COMMAND



JAN 7 1960
AEDC-TN-59-182
FC

(Title Unclassified)
STABILITY AND CONTROL CHARACTERISTICS
OF SEVEN LENTICULAR MODELS
AT MACH NUMBER 5

By
A. Anderson
VKF, ARO, Inc.

CLASSIFIED DOCUMENT

"This material contains information affecting the national defense of the United States within the meaning of the Espionage Laws, Title 18, U.S.C., Sections 793 and 794, the transmission or revelation of which in any manner to an unauthorized person is prohibited by law."

January 1960

ARO Project No. 311953

Contract No. AF 40(600)-800

CONTENTS

	<u>Page</u>
ABSTRACT	3
NOMENCLATURE	3
INTRODUCTION	5
APPARATUS	
Wind Tunnel	5
Models	5
Instrumentation	6
TEST PROCEDURE	6
PRECISION OF DATA	7
RESULTS	7
CONCLUSIONS	8
REFERENCES	8

TABLE

1. Summary of Test Configurations	9
---	---

ILLUSTRATIONS

Figure

1. Tunnel E-1, a 12 x 12-in. Supersonic Wind Tunnel	10
2. Model Photographs	11
3. Sketch of Model and Balance Arrangement	13
4. Sketches of Models	14
5. Longitudinal Characteristics of Basic Models	17
6. Longitudinal Stability and Control Characteristics	18
7. Lateral Stability and Control Characteristics	19
8. Typical Schlieren Photographs	20

ABSTRACT

Longitudinal and lateral characteristics were obtained on seven models of lenticular shape at Mach 5 and a Reynolds number of 1.5 million (based on model diameter). The effect of various control surfaces on the characteristics of the lenticular shaped body is shown. Data for a body of greater thickness-to-chord ratio and for a body with blunt edges are also presented.

NOMENCLATURE

A_b	Model base area, 0.5185 sq in.
C_A	Axial-force coefficient, $C_{A_t} - C_{A_b}$
C_{A_b}	Base axial-force coefficient, $(p - p_b) A_b / qS$
C_{A_t}	Total axial-force coefficient, $\frac{\text{total axial force}}{qS}$
C_D	Drag coefficient, $\frac{\text{drag}}{qS}$
C_l	Rolling-moment coefficient, $\frac{\text{rolling moment}}{qSc}$
C_L	Lift coefficient, $\frac{\text{lift}}{qS}$
C_m	Pitching-moment coefficient, $\frac{\text{pitching moment}}{qSc}$ (see Fig. 4 for moment reference point)
C_n	Yawing-moment coefficient, $\frac{\text{yawing moment}}{qSc}$ (see Fig. 4 for moment reference point)
C_N	Normal-force coefficient, $\frac{\text{normal force}}{qS}$
C_Y	Side-force coefficient, $\frac{\text{side force}}{qS}$
c	Model centerline chord, 8.0 in. (except for Model 6 where $c = 8.25$ in.)
M	Mach number
p	Free-stream static pressures, psia

p_o	Free-stream stagnation pressure, psia
p_b	Base pressure, psia
q	Free-stream dynamic pressure, psia
Re	Reynolds number based on model diameter of 8 in.
S	Model planform area, 50.27 sq in. (except Model 6 where $S = 53.4$ sq in.)
α	Angle of attack, deg
δ	Angle of yaw, deg

INTRODUCTION

At the request of the Air Proving Ground Center (APGC), Eglin Air Force Base, tests were conducted on seven lenticular models at Mach 5 and Reynolds number of 1.5×10^6 (based on model diameter) in tunnel E-1 of the von Karman Gas Dynamics Facility, AEDC, July 13-23, 1959. These tests were the third in a series made in support of an APGC investigation of lenticular models. The previous tests, also conducted in Tunnel E-1, are reported in Refs. 1 and 2.

The primary objective of this test series was to obtain experimental data on the stability characteristics of the basic lenticular body equipped with various control surfaces.

APPARATUS

WIND TUNNEL

Tunnel E-1 is an intermittent, supersonic wind tunnel with a 12-in. square test section (Fig. 1). The top and bottom walls are flexible plates which are manually positioned with screw jacks to produce Mach numbers ranging from 1.5 to 5. Stagnation pressures from sub-atmospheric to four atmospheres are automatically regulated by throttling the flow from a high-pressure, dry-air, storage tank. Heating coils about the storage tank provide stagnation temperatures between 70 and 129° F, depending upon test conditions. A large vacuum sphere coupled to the wind tunnel diffuser permits operation at low density levels. The angle-of-attack sector, which pitches the model in the horizontal plane, covers a range from about -5 to +15 deg. The absolute humidity of the tunnel air is normally below 0.00015 lb of water per lb of air. During these tests stagnation temperatures varied from 70 to 90° F.

MODELS

The seven models and sting support were designed by APGC to accommodate an existing VKF internal balance. Model construction was of aluminum with polished surfaces. Photographs of several models are presented in Fig. 2, and a typical model-balance installation is illustrated in Fig. 3.

Manuscript released by author December 1959.

Model details are presented in Fig. 4. Model 1 had eight stabilizing surfaces (herein referred to as 'flaps') derived by hinging sections of the exterior surfaces as shown in Fig. 4a. These sections were pinned to the model base and were removable so that flap deflection arrangements of 0, 5, and 10 deg could be obtained without removing the model from the sting support. This model was also tested with these sections set out one quarter inch from the model surface (flaps-open configuration). Model 2 had twin tail booms (Fig. 4b) and was tested with and without 20-deg wedges which were glued, in various combinations, to the boom surfaces. The elevon-like surfaces of Model 3 (Fig. 4c) had fixed deflection angles of 0 and -10 deg. Model 4 (Fig. 4d) had a drooped nose and was also tested with a small, 22-deg wedge (Tab) located on the model centerline just aft of the nose breakline. Model 5 (Fig. 4e) is simply the basic lenticular shape with the addition of vertical fins. All the models except models 6 and 7 had the same basic body shape. Models 6 and 7 (Fig. 4f) had a greater body thickness ratio, and in addition, Model 7 had a blunt edge radius.

The balance locknut cavity of each model (see Fig. 3) was filled with cotton wool and sealed over by a fairing of dental plaster.

INSTRUMENTATION

The force and moment measurements were made with VKF internal balance E1-B6I-8. The gage outputs from the balance were measured with 400-cps force readout units. These units are a null-balance servo system having both a dial indicator and an electrical digitizer serving as the gage input to an ERA 1102 computer.

Absolute base pressure was measured with a 1-psi differential transducer which had a vacuum for a reference pressure. The transducer output was measured with a d-c millivolt digitized recorder, which also served as the input to the computer.

Other data items, such as angle of attack and stagnation temperature and pressure, were measured, digitized, and automatically recorded.

TEST PROCEDURE

Data were obtained at Mach 5, at a constant Reynolds number, based on model diameter of 8-in., of approximately 1.5 million, and at angles of attack and yaw from -5 to +15 deg. For the yaw data, the model and balance were rolled 90-deg from the pitch plane.

Pitching and yawing moments were measured about the moment reference point (see model sketches, Fig. 4), and rolling moments were taken about the model centerline. The angles of attack and yaw were corrected for deflections of the sting support caused by air loads on the model. Data were obtained for the model configurations as summarized in Table 1.

PRECISION OF DATA

The uncertainties in the basic measurements, listed below, were determined from the balance calibration data, the tunnel airflow calibration data, and the known precision of pressure measuring instrumentation.

Nominal M	Calibrated M	P ₀ psia	q psia	P _b psia	
5	5.01	±0.06	±0.010	±0.0008	
C _L	C _m	C _D	C _Y	C _n	C _l
±0.27 x 10 ⁻²	±0.46 x 10 ⁻³	±0.8 x 10 ⁻³	±0.6 x 10 ⁻³	±0.23 x 10 ⁻³	±0.1 x 10 ⁻³

The variation in test section Mach number along the tunnel centerline is within ±0.01, and the estimated accuracy of the sector positioning of the angle of attack is ±0.10 deg.

RESULTS

The basic force and moment coefficients for models without control surface deflection are presented in Fig. 5. Included in this figure for comparison purposes are data obtained on the basic lenticular body (Model 5 with fins removed). As these data show, the inherent instability of the lenticular body was increased by increasing the thickness ratio (Models 6 and 7). The drag increase in both cases was considerable. A significant decrease in instability with a very small drag increase was obtained, however, by adding thickness at the trailing edge of the lenticular body (Model 1). The tail-booms of Model 2 gave similar results.

Although all the model configurations tested were longitudinally unstable about the mid-chordline, a significant amount of pitch control was obtained by the flaps of Model 1 and the wedges of Model 2 (Fig. 6). The decrease in effectiveness of these controls on the leeward surface with angle of attack is shown by the data presented for

10-deg flap deflections on Model 1 and the "top only" wedge locations of Model 2. These data (Fig. 6) also show that the elevons of Model 3 did not affect the stability level of the basic lenticular body and produced negligible pitch control. The drooped nose of Model 4 produced a trim lift coefficient of 0.03 (trim angle about 4 deg); the effect of the small tab on these results was negligible.

All the model configurations were laterally stable as shown in the typical data given in Fig. 7a. These data show the directional control obtained, by asymmetrically increasing drag, on Models 1, 2, and 3. Deflecting the elevons on Model 3 reduced directional stability and produced only small control moments. The maximum roll control was obtained by the wedges of Model 2 (Fig. 7b); however, all the roll control methods were effective.

Typical schlieren photographs of each model are given in Fig. 8. The photographs of Model 1 show an increase in flow separation at the trailing edge obtained with flap deflection. A photograph of Model 5 (less fin) at about 10-deg angle of attack is included to show the extent of the separation on the upper surface at this condition.

CONCLUSIONS

All configurations were longitudinally unstable and directionally stable.

Several methods for obtaining longitudinal and lateral control were effective.

REFERENCES

1. Anderson, A. "Aerodynamic Test Results of Two Configurations of a Proposed Bomber Defense Missile at Supersonic Speeds." AEDC-TN-58-72, October 1958. (Secret)
2. Anderson, A. "Stability Tests of Three Lenticular Models at Supersonic Speeds." AEDC-TN-59-99, September 1959. (Secret)

TABLE 1
SUMMARY OF TEST CONFIGURATIONS

MODEL 1	FLAP CONFIGURATION (See Fig. 4a)	DATA		PLANE	
		α	ψ	α	ψ
	T e B All 0°	X	X		X
	T e B All 5°	X	X		X
	T e B All 10°	X	X		X
	T All 0°, B All 10°	X	X		X
	T All 0°, B All 5°	-	X		-
	T All 5°, B All 10°	X	X		X
	T ₁ - 5°, B ₁ - 5°	X	X		X
	T ₁ - 10°, B ₁ - 10°	X	X		X
	T ₁ - 10°, B ₁ - 5°	X	X		X
	T ₁ - 5°, B ₁ - 10°	X	X		X
	T ₁ - 5°, B ₁ - 5°	X	X		X
	T ₁ - 10°, B ₁ - 10°	X	X		X
	T ₃ - 10°, B ₂ - 10°	-	X		-
	T ₄ - 10°, B ₁ - 10°	X	X		X
	T ₁ - 10°, B ₁ , B ₄ - 5°	X	X		X
	T ₁ , T ₄ - 10°, B ₁ , B ₄ - 10°	X	X		X
	T ₁ , T ₂ - 5°, B ₁ , B ₂ - 5°	X	X		X
	T ₁ , T ₂ - 10°, B ₁ , B ₂ - 10°	X	X		X
	T ₁ , B ₁ - 10°, T ₂ , B ₂ - 5°	X	X		X
	T ₁ , B ₁ - 10°, T ₂ , T ₃ , B ₂ , B ₃ - 5°	-	X		-
	T ₁ , T ₂ , T ₃ - 5°, B ₁ , B ₂ , B ₃ - 5°	-	X		-
	All Flaps Removed	-	X		X

MODEL 2	WEDGE LOCATION (See Fig. 4b)	DATA		PLANE	
		α	ψ	α	ψ
	NONE	X	X		X
	T-2, B-2	X	X		X
	T-1, B-2	X	X		X
	T-1, 2	X	X		-
	B-1, 2	X	X		X
	T-1, 2; B-1, 2	X	X		X

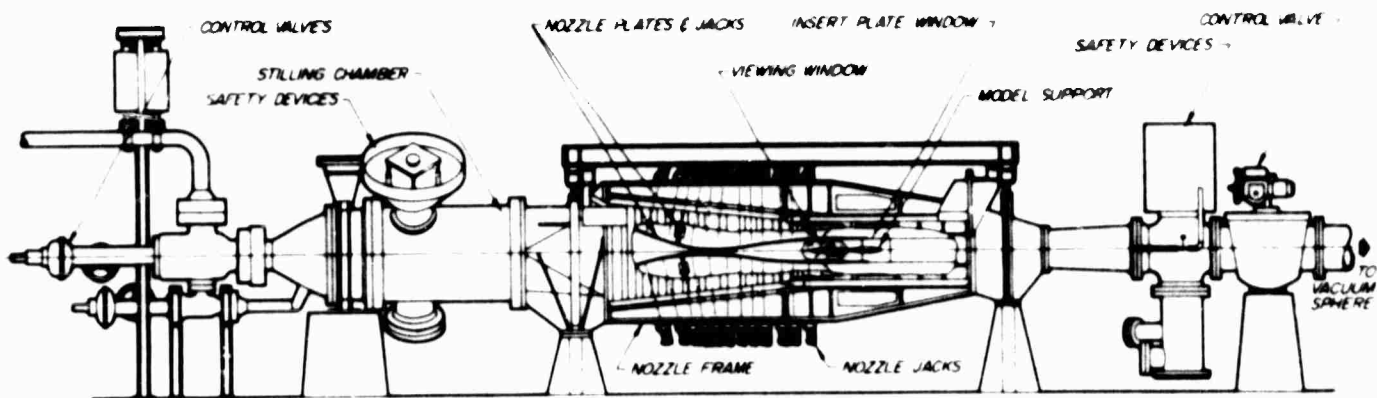
MODEL 3	ELEVON CONFIGURATION (See Fig. 4c)	DATA		PLANE	
		α	ψ	α	ψ
	R - 10°, L - 10°	X	X		X
	R - 0°, L - 10°	X	X		X

MODEL 4	CONFIGURATION (See Fig. 4d)	DATA		PLANE	
		α	ψ	α	ψ
	Without Tab	X	X		X
	With Tab	X	X		X

MODEL 5	See Fig. 4e " (No Flaps)	DATA		PLANE	
		α	ψ	α	ψ
	See Fig. 4e	-	X		X
	"	X	X		-

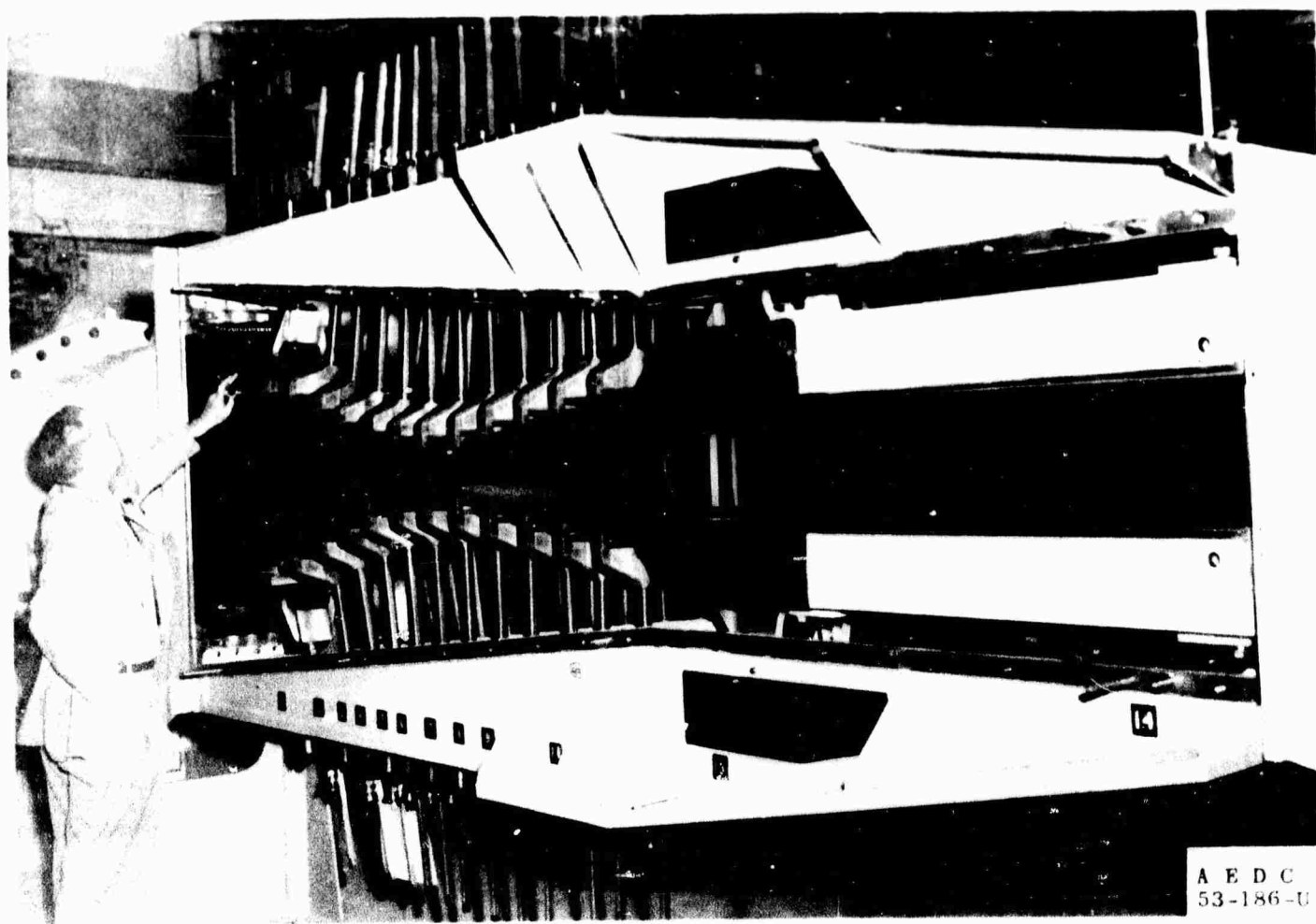
MODEL 6	See Fig. 4f	DATA		PLANE	
		α	ψ	α	ψ
	See Fig. 4f	X	X		-
	"	X	X		-

LEGEND: T - Top
 B - Bottom
 L - Left
 R - Right
 O - Flaps Open Config.
 C - Flaps Closed Config.



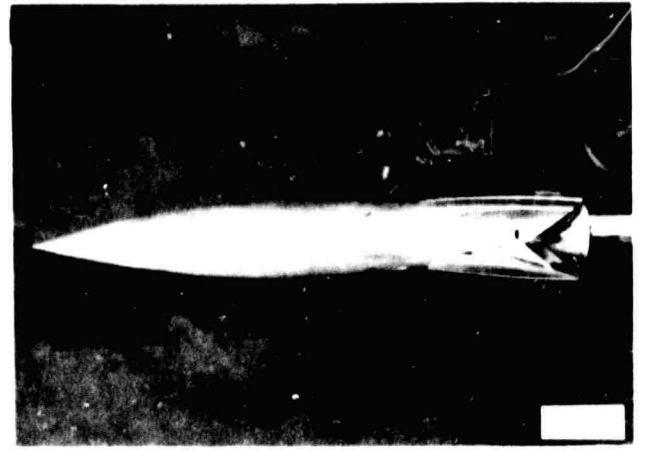
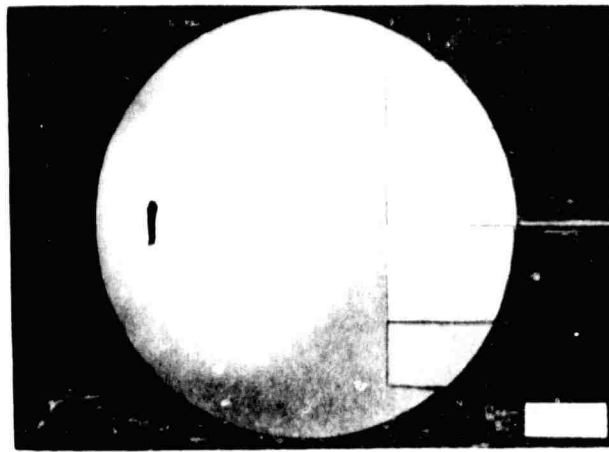
0 3 6
FEET

Assembly

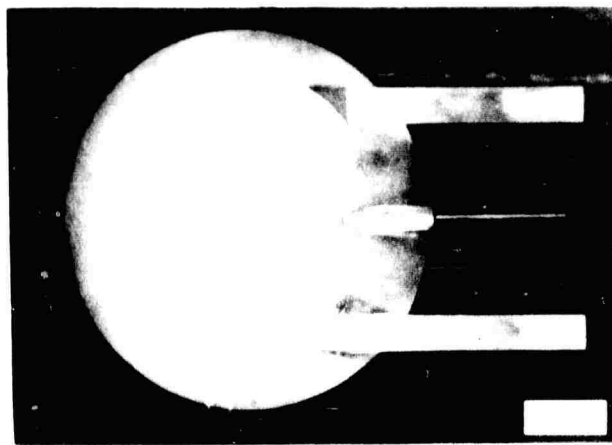


Nozzle and Test Section

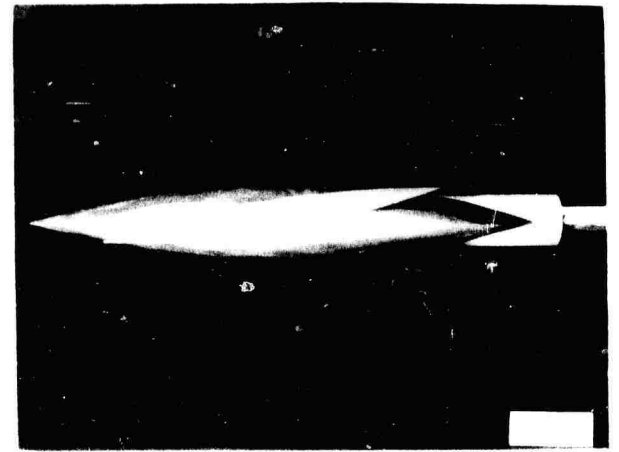
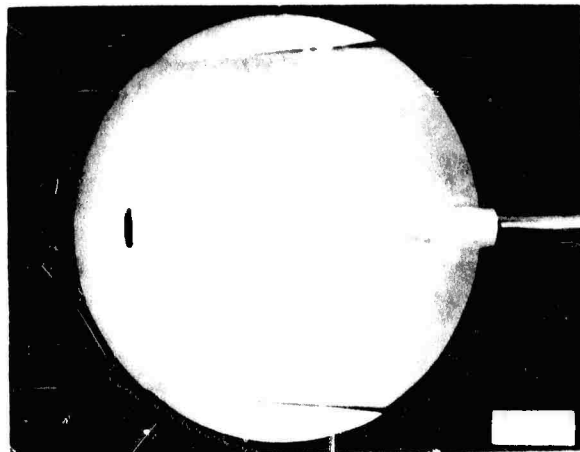
Fig. 1 Tunnel E-1, a 12 x 12-in. Supersonic Wind Tunnel



Model 1

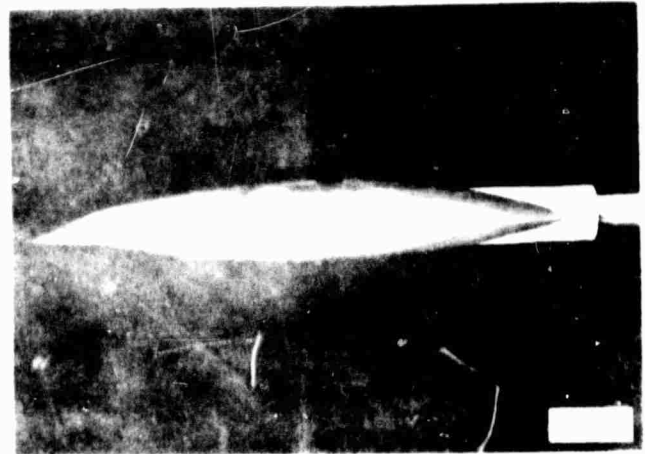
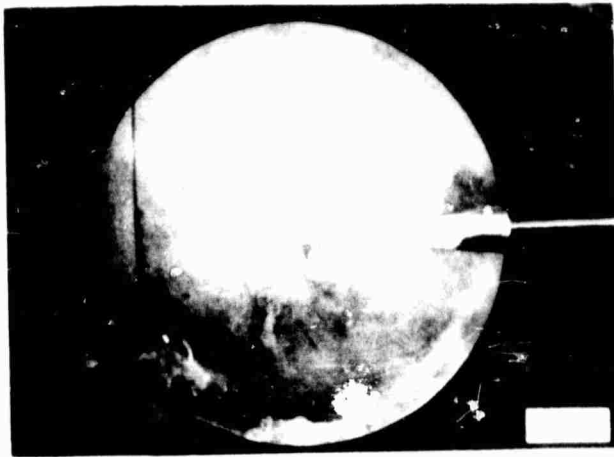


Model 2

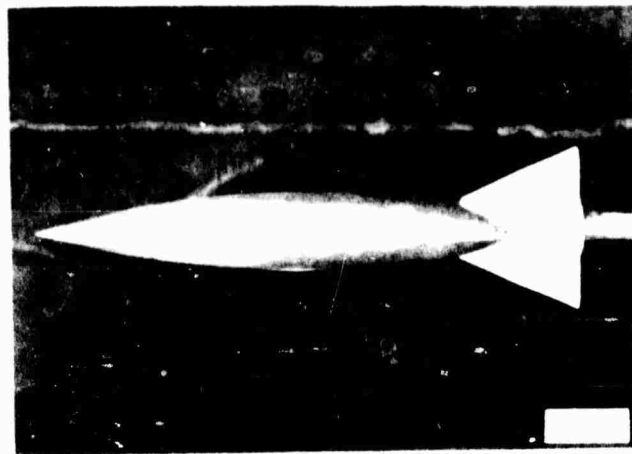


Model 3

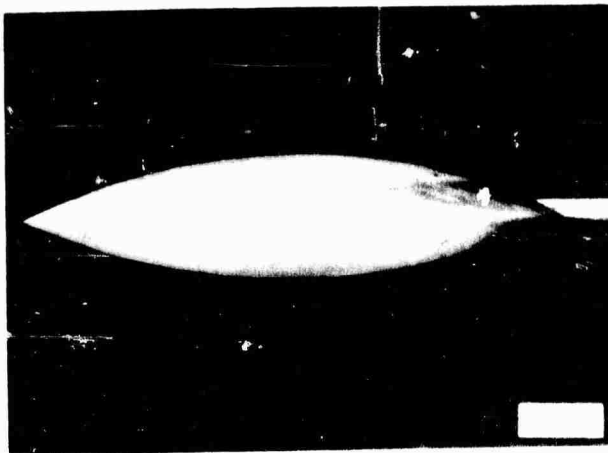
Fig. 2 Model Photographs



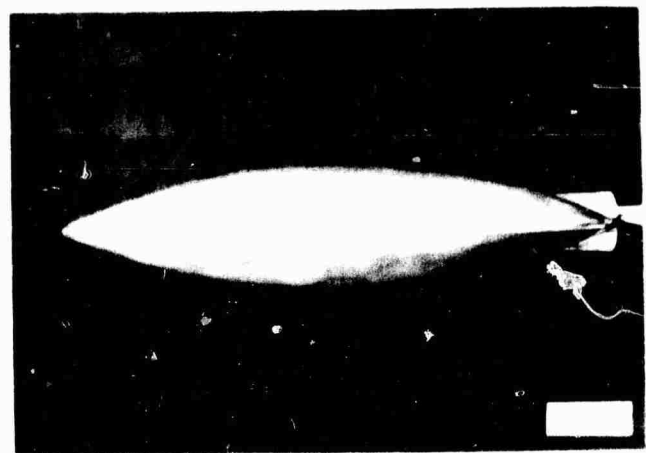
Model 4



Model 5



Model 6



Model 7

Fig. 2. Conclusions

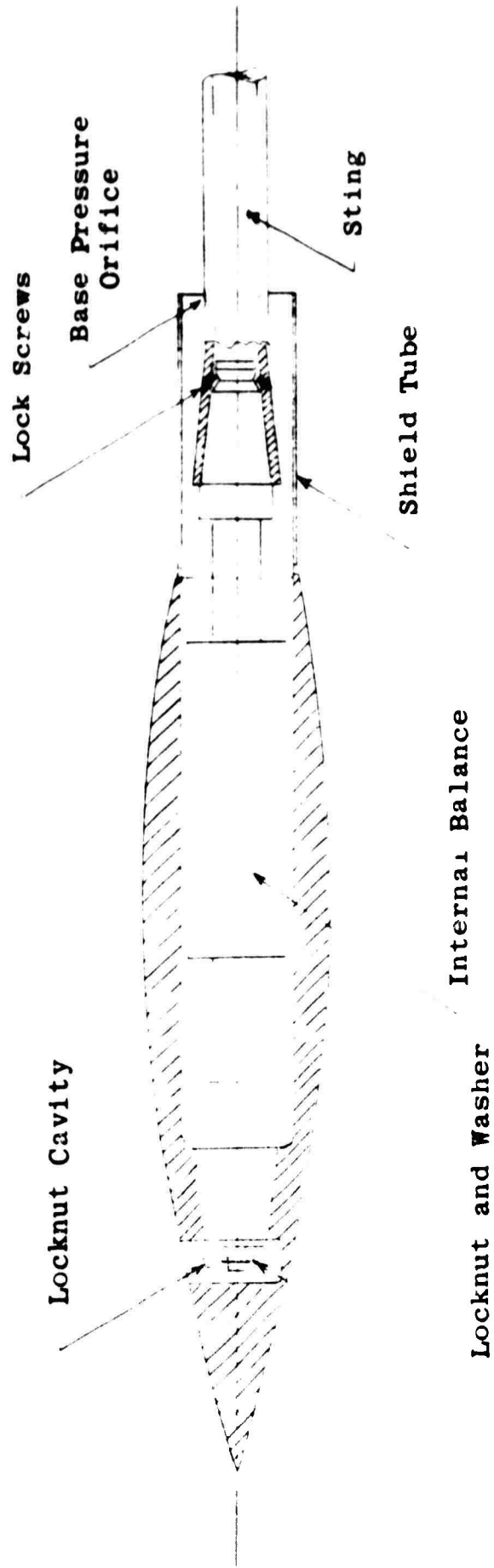
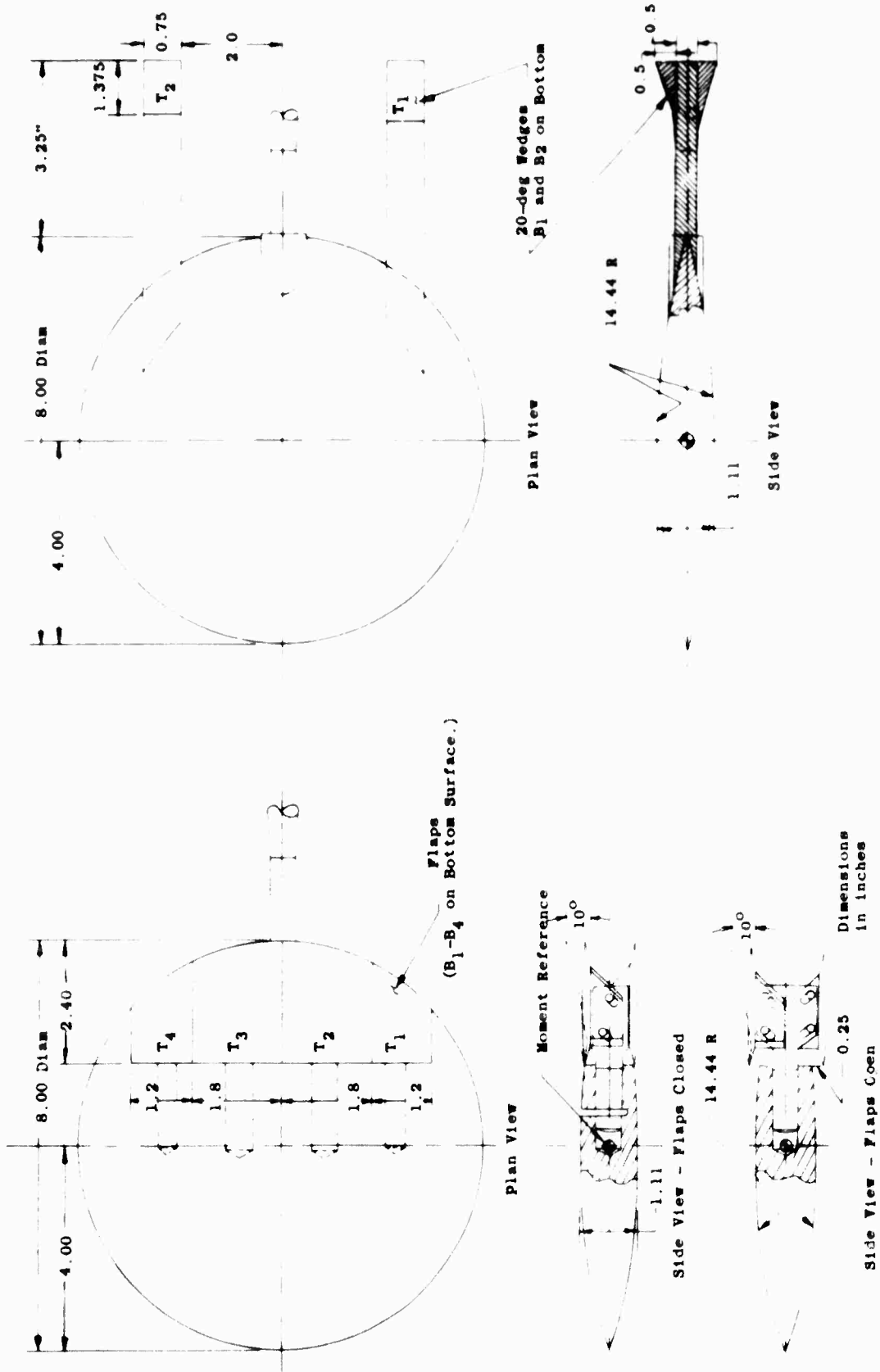


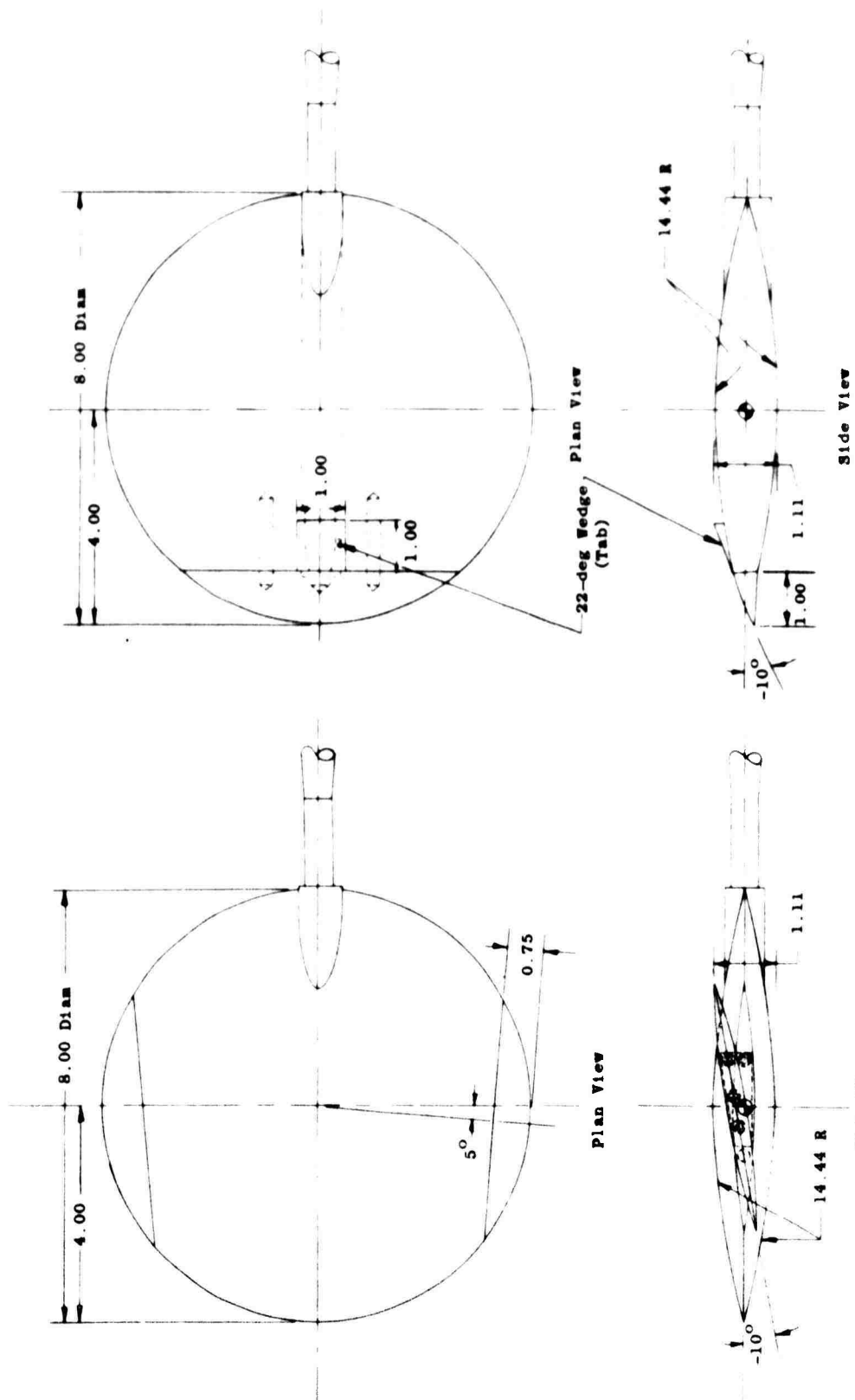
Fig. 3 Sketch of Model and Balance Arrangement



b. Model 2

a. Model 1

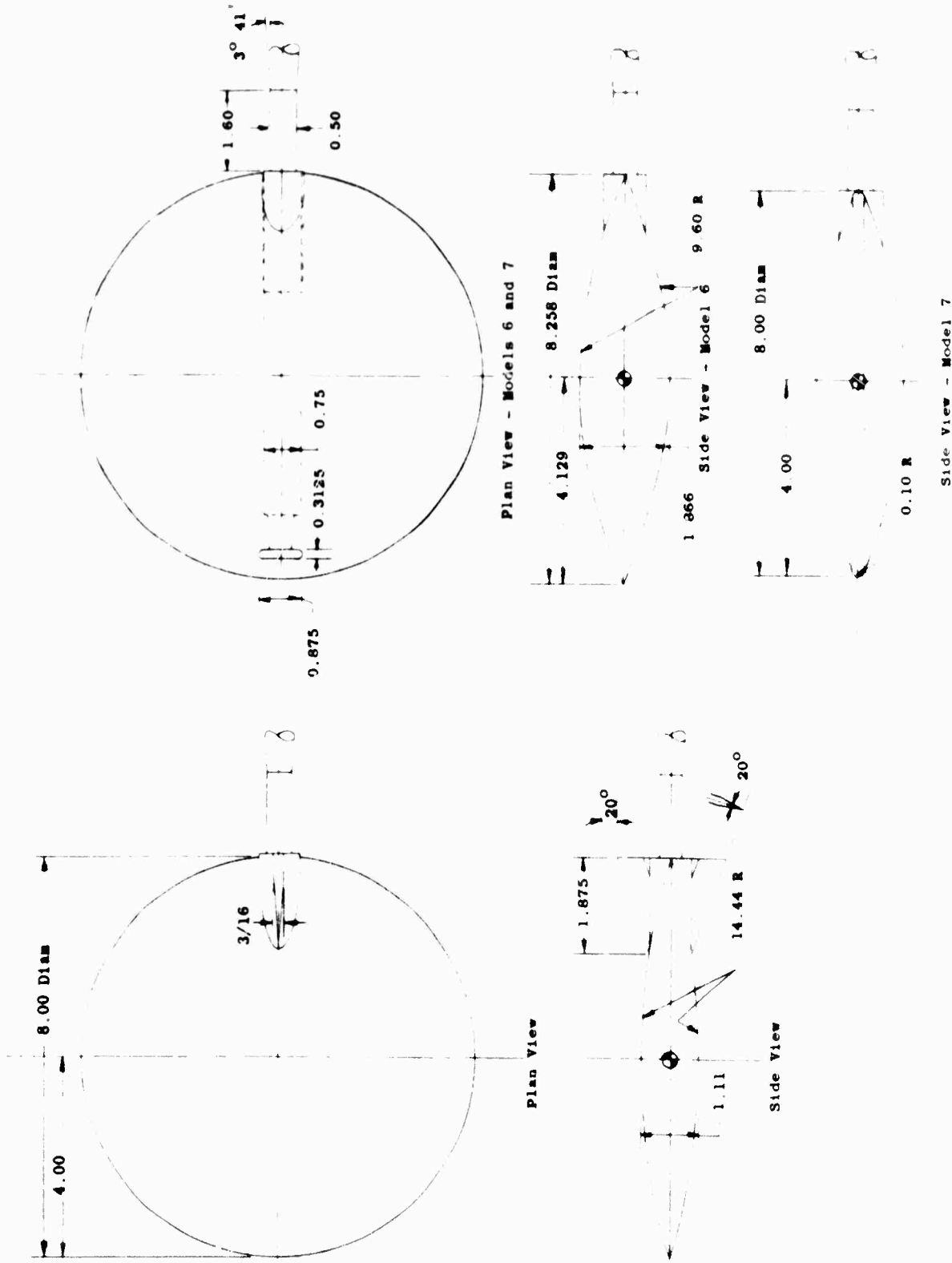
Fig. 4 Sketches of Models



c. Model 3

d. Model 4

Fig. 4 Continued



f. Models 6 and 7

e. Model 5

Fig. 4 Concluded

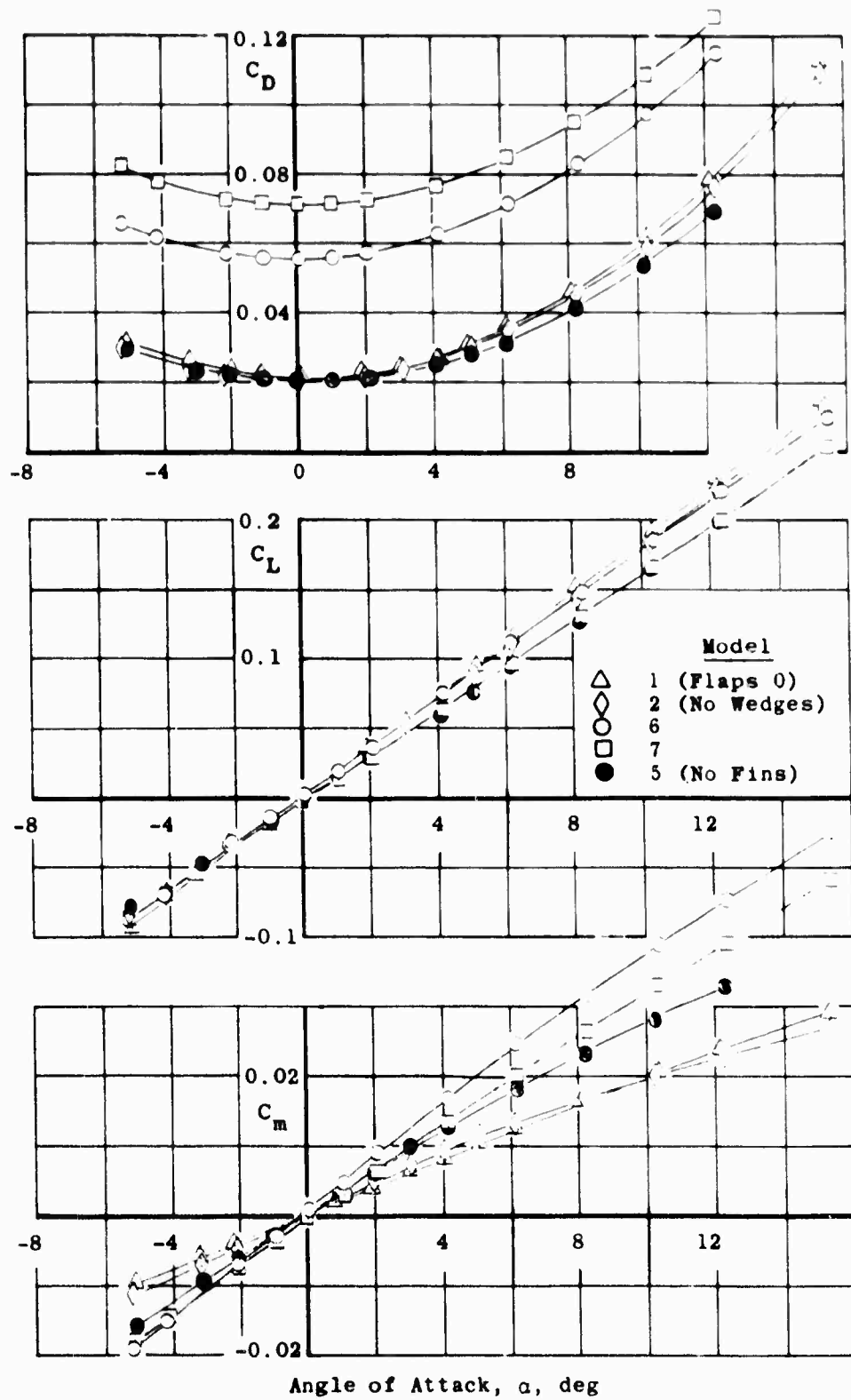


Fig. 5 Longitudinal Characteristics of Basic Models

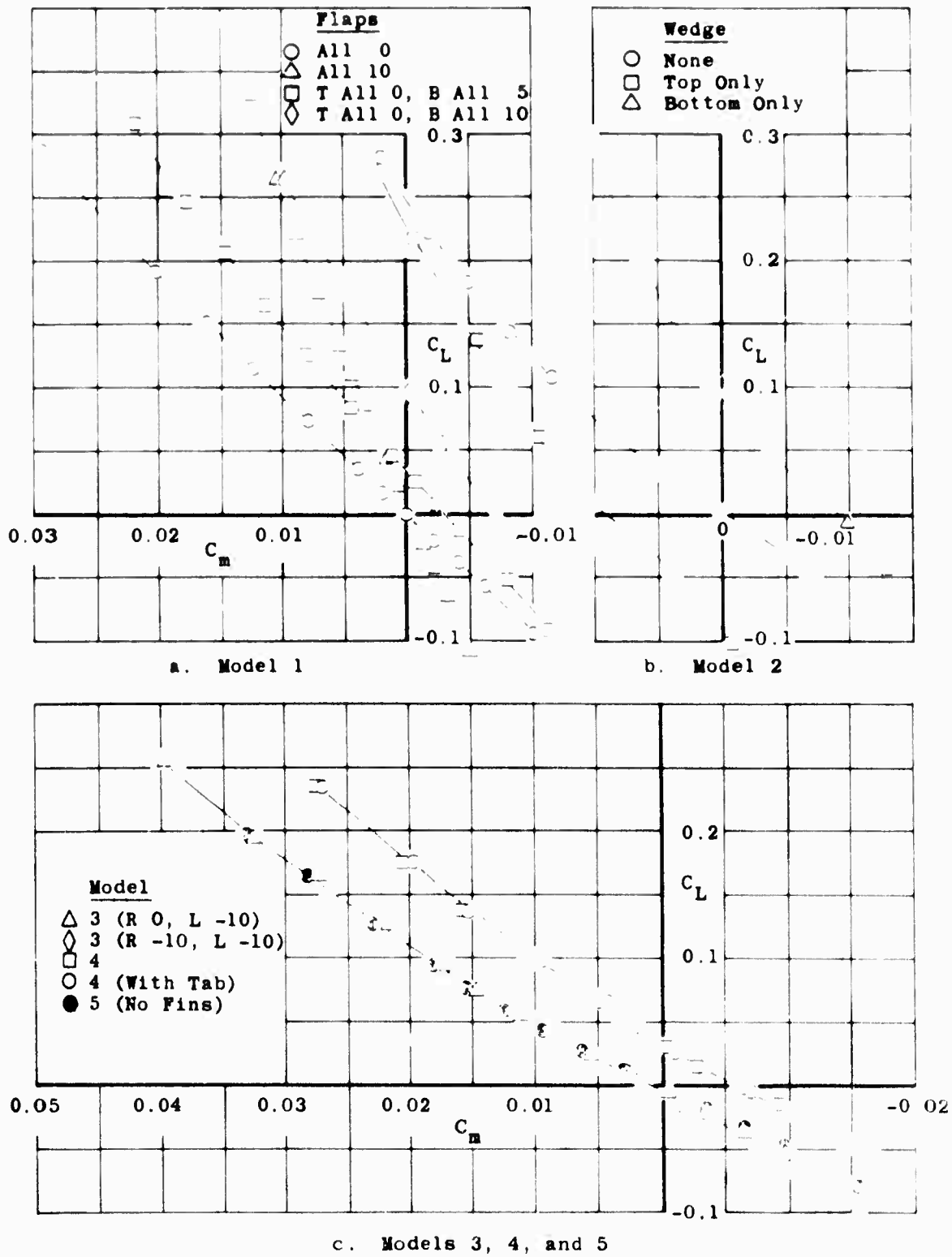
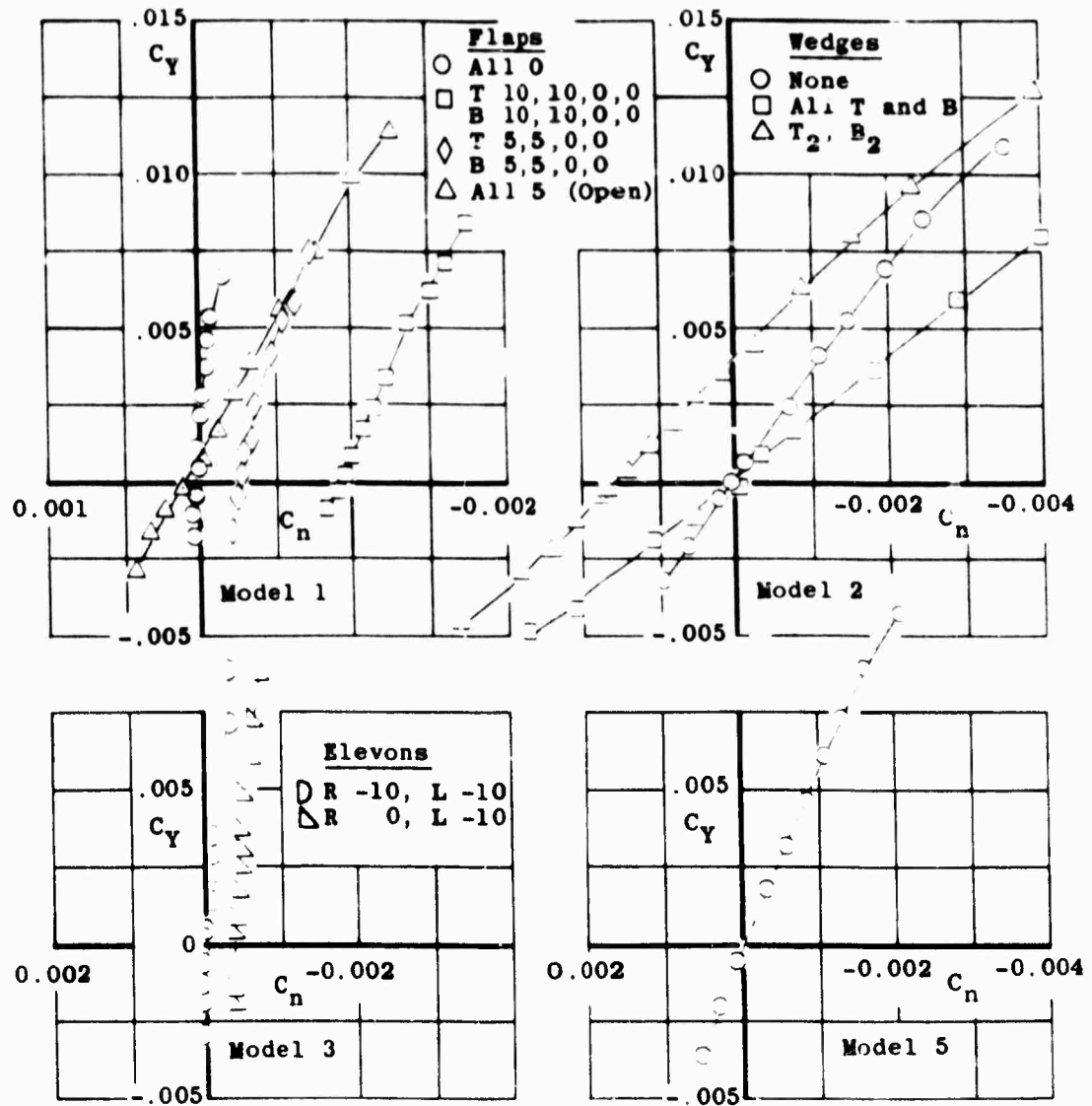
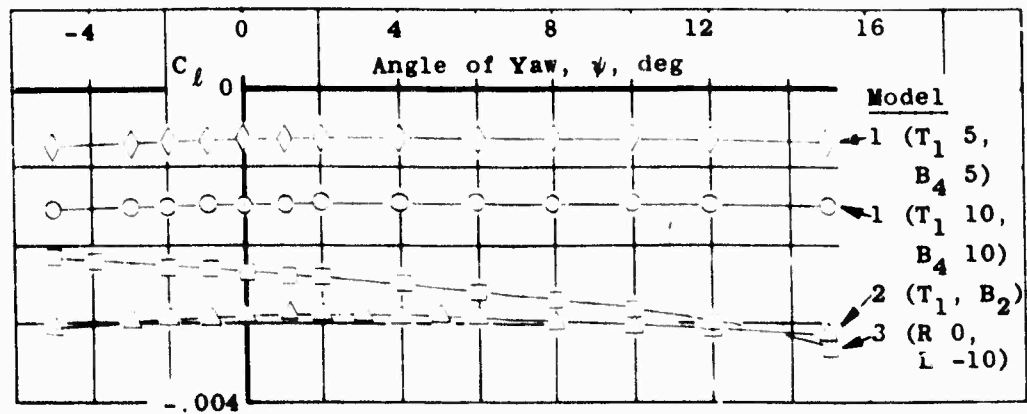


Fig. 6 Longitudinal Stability and Control Characteristics

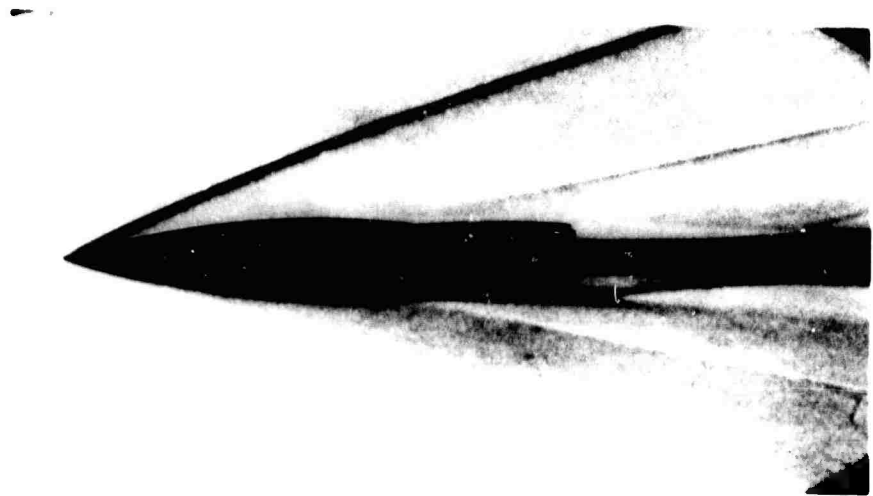


a. Directional Stability and Control

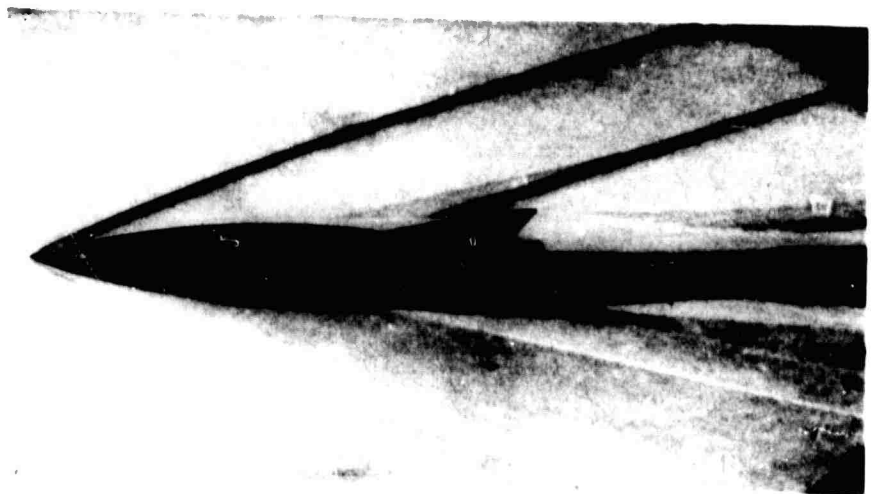


b. Roll Control

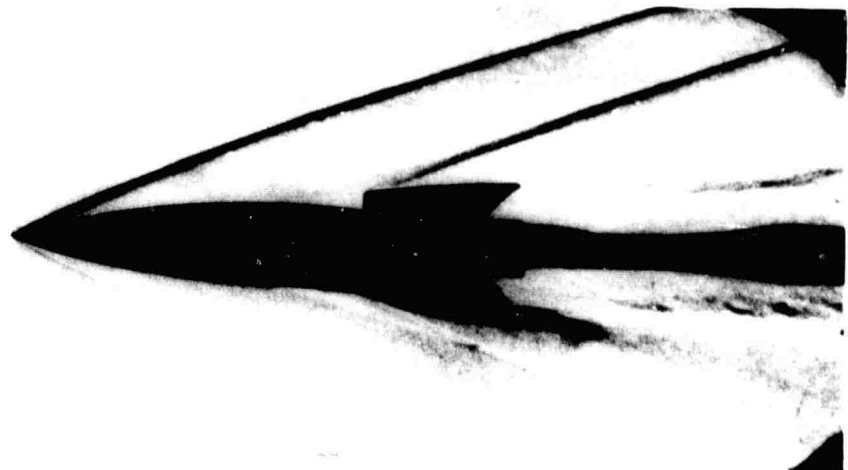
Fig. 7 Lateral Stability and Control Characteristics



All Flaps at 0



All Top Flaps 10°, All Bottom 0°



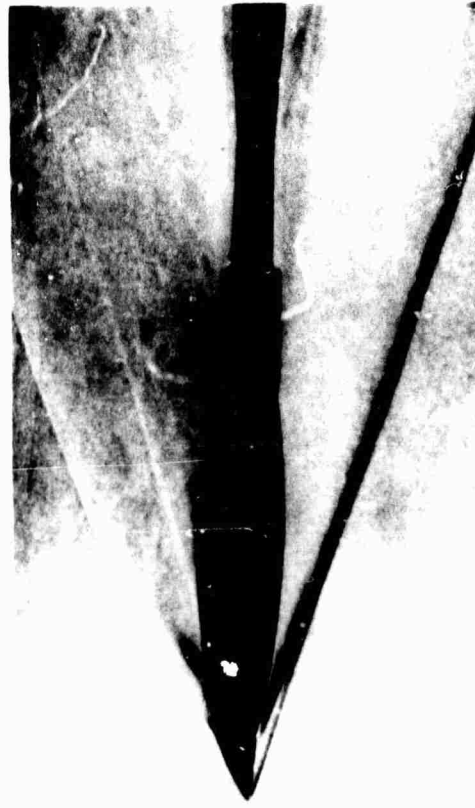
All Flaps 5, Open Configuration

a. Model 1

Fig. 8 Typical Schlieren Photographs



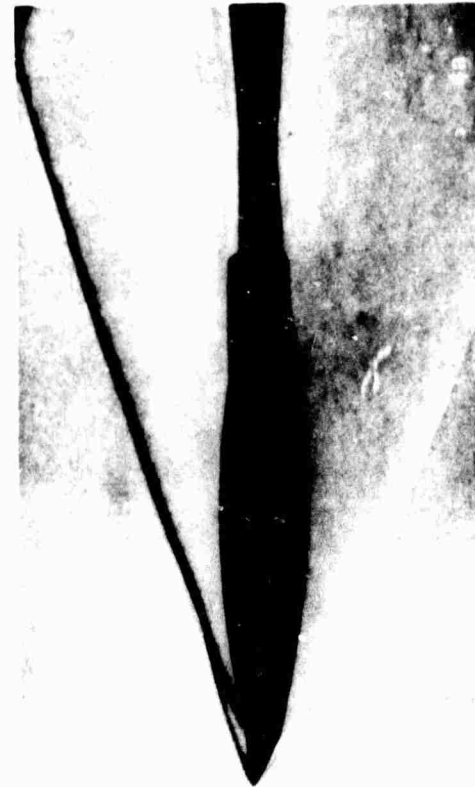
c. Model 3, Elevons at -10°



With Tab



b. Model 2, Wedges T_1 and B_1



No Tab

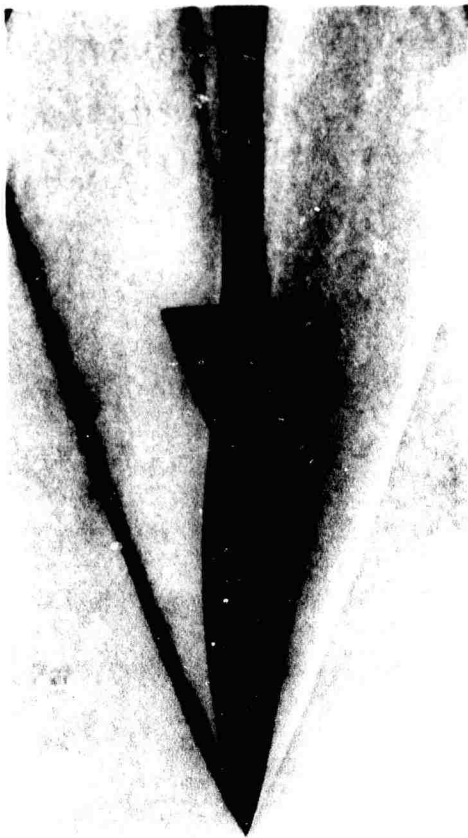
d. Model 4

Fig. 8 Continued



Without Fins, " 10

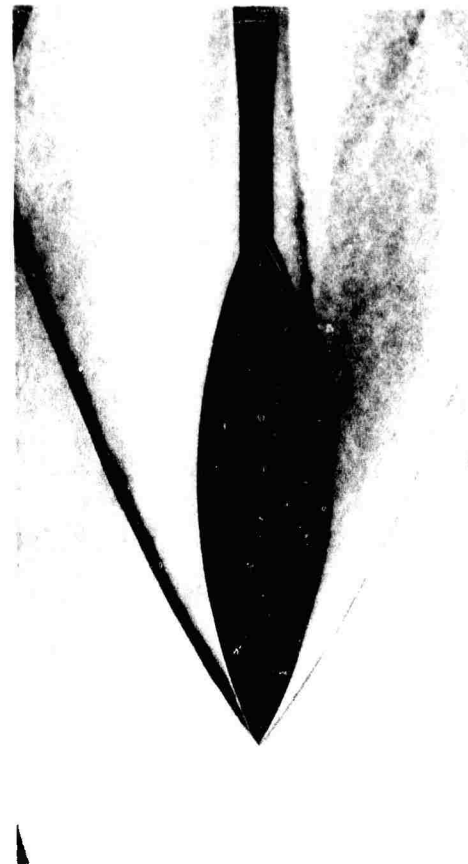
e. Model 5



With Fins



g. Model 7



f. Model 6

Fig. 8 Concluded